



# A New Paradigm to Investigate and Differentiate Formalin-Fixed Oral Malignant, Benign and Cyst tissue samples using Active Pulsed Thermography.

S.Stella Jenifer Isbella<sup>1</sup>, K.A.Sunitha<sup>2\*</sup>, K.T.Magesh<sup>3</sup> M Menaka<sup>4</sup>, P.A.Sridhar<sup>5</sup>

<sup>1</sup>Department Electronics & Instrumentation Engineering, SRM Institute of Science and Technology, Chennai, India.

<sup>2</sup>Department Electronics & Communication Engineering, SRM University, AP, India.

<sup>3</sup>Department of Oral Pathology and Microbiology, SRM Kattankulathur Dental College, SRMIST, Chennai, India.

<sup>4</sup>Head, RAMS, Indira Gandhi Centre for Atomic Research, Kalpakkam, India.

<sup>5</sup>Department Electronics & Instrumentation Engineering, SRM Institute of Science and Technology, Chennai, India.

\*Corresponding author: K. A. Sunitha, <sup>2</sup>Department Electronics & Communication Engineering, SRM University, AP, India. E-mail: [sunitha.ka@srmmap.edu.in](mailto:sunitha.ka@srmmap.edu.in)

**ABSTRACT:** Active thermography (AT) is a non-destructive testing method that has been intensively investigated for the characterization and assessment of biological and industrial materials, among other things. Passive thermal imaging is limited to distinguishing between an oral malignant, benign, and cyst based on temperature differences. The proposed work introduces the Active pulsed thermography (AT) technique to investigate ten oral malignant, benign, and cysts samples. Each specimen sample provides more physiologically relevant measures with good contrast based on the rate of change in temperature and thermal recovery time. The experimental result shows that with heating modulation, we discovered that the average rate of temperature change in the tumor ( $0.35 \pm 0.10^\circ\text{C}/\text{sec}$ ) was greater than that of benign and cyst tissue ( $0.33 \pm 0.1^\circ\text{C}/\text{sec}$ ) and ( $0.28 \pm 0.1^\circ\text{C}/\text{sec}$ ). Thermal recovery time in cancer tissue, on the other hand, was shorter ( $\tau=0.6 \pm 0.3\text{sec}$ ) than in benign tissue ( $\tau = 0.48 \pm 0.24 \text{ sec}$ ) and cyst ( $\tau=0.46 \pm 0.22\text{sec}$ ). The results are validated with the gold standard histopathology techniques. Because of its intrinsic label-free and physiology-based approach, our findings imply that Active Pulsed Thermography may be a promising tumour detection method for clinical use in the future.

**KEYWORDS:** Passive Thermography; Pulsed Thermography; Formalin-Fixed Oral samples; Thermal contrast; Histopathology; cell density; Protein; Lipids.

## 1. Introduction:

Oral cancer is sixth most frequent cancer in the world, behind lung cancer and breast cancer.

It is a severe public health issue that must not be overlooked. India has the most significant number of incidences of oral cancer, with 77000 new cases identified each year and 52000 fatalities reported. The public burden of oral cancer is enormous due to the origin of the disease and the associated morbidity. When a patient has a history of smoking, smokeless tobacco [1],

betel-quid usage, chronic alcohol misuse, untidy oral hygiene, poor nutrition, and extended viral infections such as the Human Papilloma Virus, the likelihood of developing oral cancer increases dramatically (HPV) [2]. The delayed diagnosis, oral disease, and an ineffective cure lead to a five-year survival rate of 20%. [3].

Imaging methods for cancer diagnosis such as X-ray, CT (computerised tomography), and PET (positron emission tomography) are already available, although they all include the threat of radiation exposure. While MRI (magnetic resonance imaging) gives 3D structural information, it is both expensive and time-consuming to do because of the long picture capture period. Recently, molecular imaging has gained popularity in discovering therapeutic applications [4, 5]. However, because most molecular imaging probes require the injection of fluorescent dye or targeting probes into a person, quick clinical translation is hampered by concerns about regulatory compliance and patient safety. The FDA authorized the VELscope®, a non-magnifying hand-held tool, in 2006 for direct observation of oral mucosa autofluorescence [6]. The published research results with 44 individual subjects revealed that the approach had high sensitivity and specificity in distinguishing OSCC from normal oral mucosa [7]. Future researchers hope to increase the instrument's specificity to make it more widely available for clinical use. A lesion sample is necessary for histological examination and subtyping since imaging scans are difficult to interpret in SCC diagnosis. A biopsy is frequently used to detect malignant tissues, which entails the collection of invasive tissue samples.

The intraoperative frozen section biopsy is often used to distinguish malignant tissue from normal tissue during surgery. Manually viewing slides stained with H&E and examined by pathologists for disease diagnosis is time-consuming and labour-intensive. Since these methods take longer (say, 48 hours) for pathology results to arrive, they are more expensive [8]. Due to manual error and false-negative results, there is a need for a device to diagnose the resected tissue along with the margins rapidly and accurately. Since the pathological study of removed tissue can take several days, and if the margins are positive, a second surgery to remove additional tissue is required. The double procedure raises the risk of infection, raises the treatment expense, and lowers the patient's and surgeon's morale.

Furthermore, thermal imaging has been utilised for many years to examine medical diseases involving heat changes in the body or skin without extra sensors [9-10]. Thermography was first used as a portable non-destructive commercial inspection method to find hidden faults in hard-to-reach areas [11]. Thermography techniques have proven helpful in diagnosing breast cancer without the need for fluorescent dyes [12-13]. Thermographic scans reveal temperature distribution concerning the targeted tissue's function, physiology, and metabolic activity. The emissivity, underlying blood supply, environmental factors, and the thermal state of a tumor

surrounded by healthy tissue are all determined by the temperature of the skin's surface. However, because temperature changes are frequently less than 1.5 degrees Celsius, this passive infrared camera modality is subject to false results and low sensitivity [14-15]. The most extensively used active approach of infrared thermographic (NDT & E) is pulsed transient and lock-in thermography [16]. The specimen surface is periodically heated (from ms to s) by multiple heating sources in pulsed transient thermography. An infrared camera captured the resulting thermal transient at the surface. The thermal and physical qualities of the material and its thickness influence the duration of the heating pulse [17]. When there is a subsurface fault or feature, heat transmission into the sample is disrupted, resulting in a temperature differential at the surface that may be detected using an infrared system. [18,19]. We anticipate that Active Pulsed Thermography-controlled heating provides more excellent contrast between oral cancer, benign, and cyst tissue to address these constraints. This distinction is likely owing to changes in the temperature state and thermo-physiological features of the diseased tissue, such as cell density, which may result in divergent patterns in response to well regulated thermal modulation. The contrast in our method, on the other hand, was related to the qualities of cell density, and substances such as protein and lipid are responsible for tissue heating and thermal properties. The technology can also be used as an auxiliary means to diagnose pathology. This approach is quick and fast and has a wide variety of applications in the medical field. As far till now, no comprehensive investigation has been conducted on the continuous application of heat modulation for tumour margin detection. It is the first time that active pulsed thermography has been utilised to study formalin-fixed oral tissues that we are aware of, and the results are encouraging.

The following sections are organized as follows. Firstly, oral cancer and basics of Active thermography are introduced in [Section 1](#). Next, the experimental study of each oral tissues sample using an active pulsed thermography technique is reviewed under [Section 2](#). Results and discussion are evaluated in [Section 3](#). After that, the results validated with immunohistopathology and a conclusion is presented in [Section 4](#).

## **II MATERIALS AND METHODS**

Ten oral cancer, benign, and cyst specimens were collected from 15 individual subjects between March 2019 and May 2020 for this investigation. Each subject gave written consent for their tissue to be utilized in research. The procedures are carried out following the guidelines of the Helsinki Declaration. The Obtained tissue is cut into thin slices with a dimension of 1.5cm X 1.2 cm X 0.3 cm and preserved in formalin.

### **2.1 ACTIVE PULSED THERMOGRAPHY EXPERIMENTAL STUDY**

A short pulse of energy is given to the surface of the specimen in pulsed thermography (PT), as seen in Fig 1. Figure 2 shows the different formalin-fixed tissues taken for the experimental study. Figure 1a shows the experimental set-up of Pulsed thermography in IGCAR, Kalpakkam. FLIR x6540sc IR camera is used for the analysis. The heating pulse causes the specimen to emit thermal waves of various frequencies

The rate of change in surface temperature (i.e. temperature contrast) is recorded using a thermal infrared camera. As additional energy is injected into the sample, the dose of radiation released from the surface (reflection mode) is tracked over time using an infrared camera. Infrared radiation is detected at 3–5 microns, with a frame rate of 50 Hz being ideal. Two 1600 W xenon flashlights were used in the APT testing. The flash lasted less than 2 milliseconds. The temperature of the material varies fast after an initial thermal disturbance because the thermal front propagates beneath the surface of the material, as well as because of radiation and convection losses, and the thermal front propagates under the surface of the material. When examining the surface temperature, deficiencies show as patches of varying temperatures about a nearby region due to the presence of the defect. Thermal diffusion happens when the heat is applied, and the IR camera detects the ensuing thermal profiles on the object's surface. The dynamic thermal diffusion process is the key to the contrast obtainable by this technique and is described by the equation (1) for thermal conduction for the temperature  $T(x, t)$

$$T(x, t) = \left[ \frac{q}{\sqrt{\pi \rho c k t}} \exp\left\{-\frac{x^2}{4\alpha t}\right\} \right] \text{-----Eq(1)}$$

$$T(0, t) = \frac{q}{\sqrt{\pi \rho c k t}} \text{-----Eq(2)}$$

Where  $\alpha$  is the thermal diffusivity ( $=\rho c$ ),  $\lambda$  is the thermal conductivity,  $\rho$  is the density, and  $c$  is the specific heat capacity. The heat source is given by  $q$  (absorbed power density in  $W/m^3$ ). APT is the determination of a sample surface & 2D thermal radiation after it has been excited.

The resultant surface temperature due to a defect at a depth  $L$  given by

$$T(x, t) = \left[ \frac{q}{\sqrt{\pi \rho c k t}} \left[ 1 + 2 \sum_{n=0}^{\infty} R^n \exp\left\{-\frac{n^2 L^2}{\alpha t}\right\} \right] \right] \text{-----Eq(3)}$$

Where  $R$  is the reflection coefficient, the reflection from the tissue samples gives a thermal mismatch between the material and the defect.

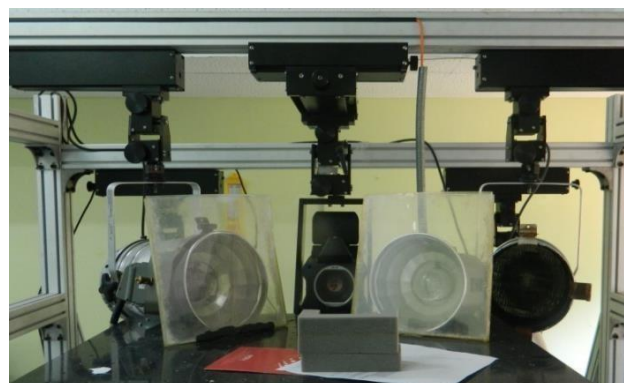
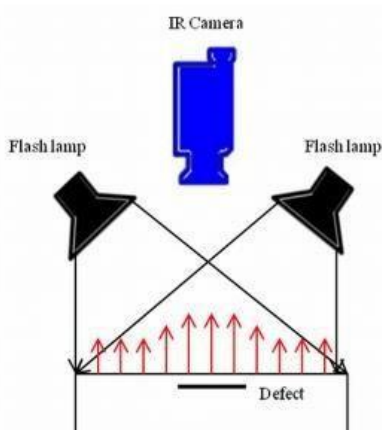


Figure 1a: Schematic Diagram of Pulsed Thermography Figure 1b: Experimental Set-up of Pulsed Thermography in IGCAR, Kalpakkam



2a. oral malignant      2b.oral Benign      2c. Oral Cysts

Figure 2a-2c The formalin –fixed oral malignant (2a), benign(2b) and cyst(2c) tissue sample for the experimental study with the dimension of 1.5cm X 1.2 cm X 0.3 cm

### III. RESULTS & DISCUSSION

#### 3.1 Thermal conductivity based on cell Density of the tissue sample:

Figure 3 explains the thermal contrast obtained after the pulse excitation. The different forms of pulsed excised tissues were labelled as 1, 2, 3 where 1 is the benign tissue sample(formalin-fixed), 2 is the malignant tissue sample (formalin-fixed), and 3 is the cyst sample (formalin-fixed). The flattened surface of the tissues were considered for the selection of ROI

. The temperature distribution on the flat surface region gives better variation in the result compared to uneven surfaces in the tissue. In addition to measuring the surface temperature response after delivering pulse thermal energy to each specimen .while recording it, the thermal conductivity of the sample varied based on the natural element present in the host material. Heat travels longer through biological tissues for higher cell density, whereas heat travels shorter through biological tissues with lower cell density. The amount of energy reflected from the surface contact calculates the change in the biological tissue's thermal effusivity. So, the temperature in the tumour region (ROI 2) significantly contrasts with neighbouring regions during the heating phase. Figure 4a illustrates the time peak recorded for cancer, benign, and cyst tissue samples.  $T(\text{Speak} - \text{Initial}) = 0.28 \pm 0.50$  °C for cancer and  $T(\text{Speak} - \text{Initial}) = 0.26 \pm 0.46$  °C for benign tissue are plotted in figure 4a. It demonstrates the maximum temperature difference after the temperature reaches the peak. The findings reveal that changes in physiological parameters of tissue samples and heating modulation enhance the difference in temperature between cancer, benign, and cyst tissues.

The difference in thermal characteristics altered the rate of heat flux penetration into the sample tissue and, as a result, the surface temperature distribution, resulting in the emergence of local

"hot spots" on the surface of the sample tissue, as shown in figure 3. The resulting temperature difference curve determines the tissue's cell density and the protein, lipid, and collagen present. We chose peak sites based on the time-dependent 1D contrast slope, as shown in figure 4b. This approach involved computing the first derivative of the temperature contrast and plotting it as a function of time. The temperature response of the thermophysical properties of the biological tissue is plotted on log scale.

### 3.2 Thermal conductivity based on Protein, lipids and collagens in the tissue sample:

Besides cell density for temperature decay, the major critical contributing factors are proteins, lipids, and collagens. The figure 4a illustrates that the formalin fixation procedure eliminates free water from the sample while maintaining tissue elements such as proteins, collagens, and lipids [20-21]. Collagens, which are matrix specialized proteins, and other cellular proteins have heat conductivity in the range of  $0.2 \text{ W m}^{-1} \text{ K}^{-1}$ – $0.3 \text{ W m}^{-1} \text{ K}^{-1}$  [22]. On the other hand, Lipids have a thermal conductivity of  $0.1 \text{ W m}^{-1} \text{ K}^{-1}$ – $0.3 \text{ W m}^{-1} \text{ K}^{-1}$  [23]. The majority of heat conduction occurs between collagens, proteins, and lipids in various cellular areas once the excess hydration in the tissue is eliminated by formalin fixation. The implications of formalin fixation are expected to be more noticeable in tumours because they include more disorganization, leakier vasculature, and more water content than normal tissues. Since the malignant tissues have more no proteins than a cyst and benign the thermal conductivity is higher, and the recovery time for the malignant is shorter than benign and cyst samples.[24]

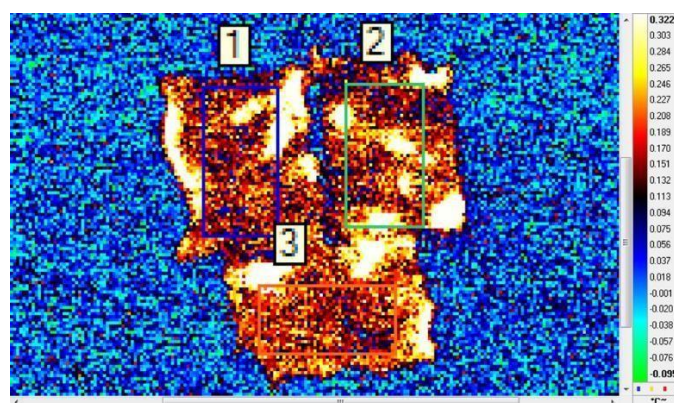


Figure 3: Formalin fixed Tissues of cancer, benign and cysts after pulse excitation 1.Benign(B); 2 Cancer(A) ; 3.Cyst(C)

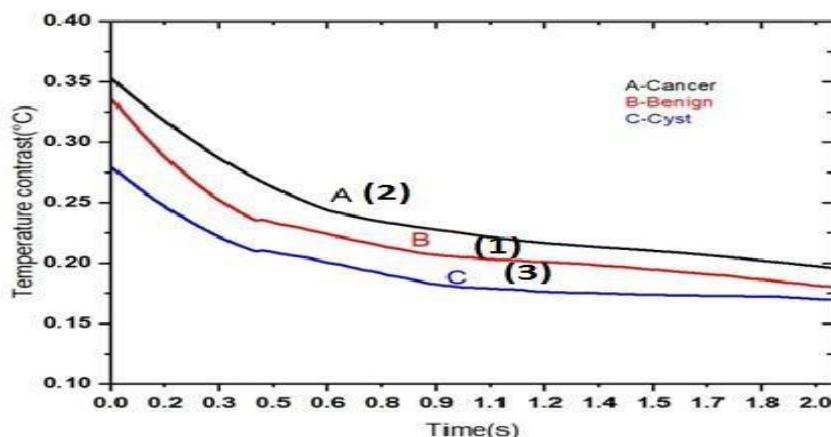


Figure 4a: Time Vs temperature Contrast Curve

### 3.3 Validation of results

This validation was done by dehydrating formalin-fixed tissues by replacing the solution with paraffin. Using a knife, the pathologist removed consistent cubical blocks of dimension 3 cm X 2 cm X 1.3cm (L × B × H) for the FFPE samples (tumor, benign, and cyst tissues). [25-27].an immunohistochemical protocol was followed to deparaffinize the formalin-fixed sample blocks. The temperature was raised in a hot air oven at 70°C for 2 hours to melt the paraffin. A xylene dip method is followed for 8 minutes and washed for 5 minutes with 100%, 95%, 70%, and 50% of different ethanol concentrations to remove any remaining paraffin wax. The wax is then removed from the sections.

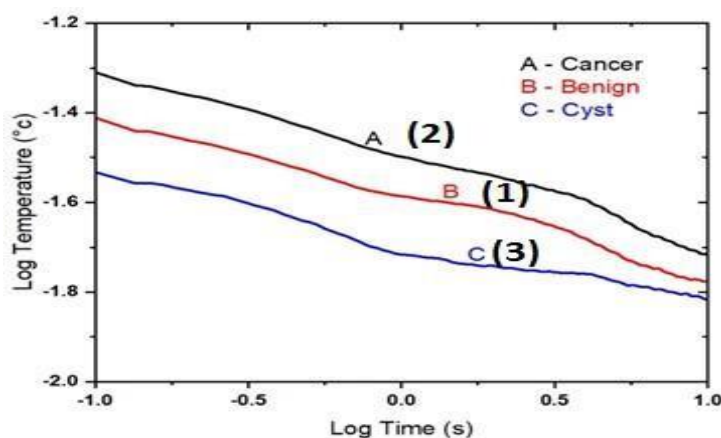


Figure 4b: Log time Vs Log temperature graph.

Finally, thin slices were impregnated on glass slides but not submerged, stained with H&E, and examined through an electron microscope [28].

### 3.4 Validation of results with Immunohistopathology:

Haematoxylin (a popular stain dye used in histology) gives a bluish hue to the nuclei, while eosin gives a pinkish-orange colour to both cytoplasm and other tissue components, as shown in Figures 5a, 5b, and 5c. The cellular differences between benign, cystic, and malignant tissues

under the microscope are examined. Cancer tissue has a very high cell density. Fast malignant/tumor cell proliferation resulted in massive increases in tissue nuclei and, in certain cases, considerably more nucleoli in oral cancer cells [29-30]. The results were confirmed by utilizing the image j software program to calculate the percentage of the nucleus of the cell cytoplasm per unit area of tissue, as shown in Table1. The table depicts that the density in the cell nucleus is very high for malignant, say, 32% when compared to the cyst at 17%. The temperature of malignant tissue reaches a maximum temperature of  $0.36 \pm 0.60$  °C/sec explicit that malignant has high proteins /cell density is more significant when compared to cyst and benign, as shown as bar diagram in figure 6a-6c.

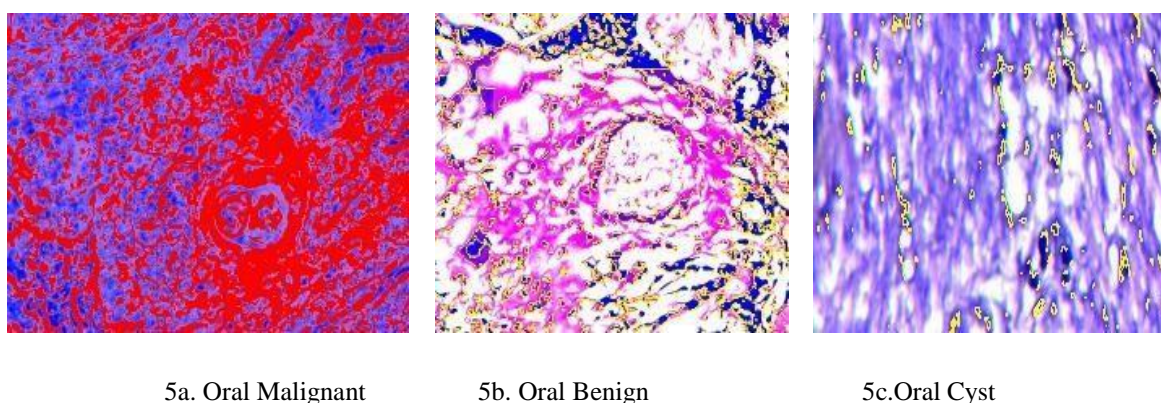


Figure 5a-5c: H& E stained microscopic slides of malignant, benign & cyst.

**TABLE1**  
EVALUATION REPORT ON H-E STAINED IMAGES [31]

	Malignant	Benign	Cyst
Cell nucleus	32.0078%	27.987%	17.11%
Cytoplasm	21.043%	48.013%	45.890%
Non-Stained areas	46.9492%	24%	37%
Rate of temperature change	$0.35 \pm 0.10$ °C/sec	$0.33 \pm 0.1$ °C/sec	$0.28 \pm 0.1$ °C/sec
Recovery time	$0.6 \pm 0.3$ sec	$0.48 \pm 0.24$ sec	$0.46 \pm 0.22$ sec

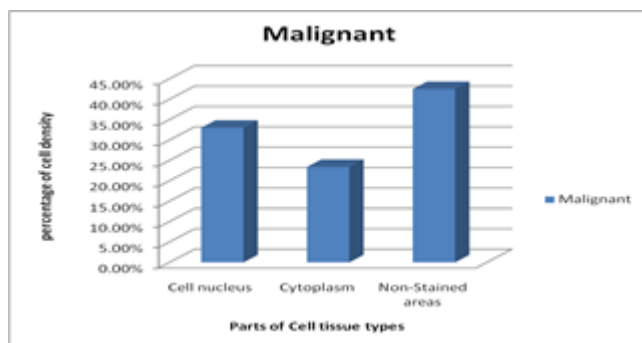


FIGURE 6a: Analysis of cell density in Formalin Fixed Malignant tissues.

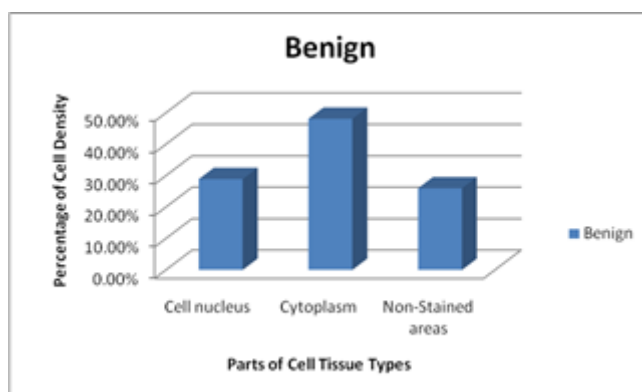


FIGURE 6b: Analysis of cell density in Formalin Fixed Benign tissues.

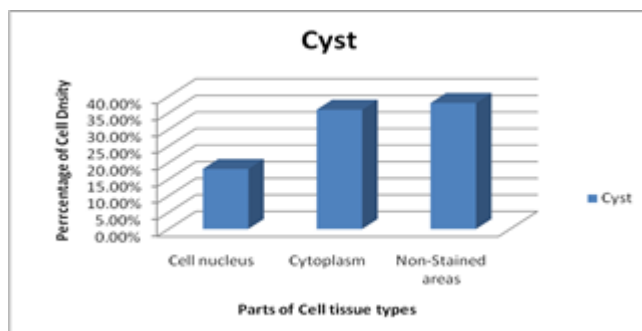


FIGURE 6c: Analysis of cell density in Formalin Fixed Cyst tissues.

The table1 depicts that the density in the cell nucleus is very high for malignant, say, 32% when compared to the cyst at 17%. The temperature of malignant tissue reaches a maximum temperature of  $0.35 \pm 0.1$  °C/sec explicit that malignant has high proteins /cell density is greater when compared to cyst and benign. Based on the thermal conductivity of protein, lipids, and collagen, the rate of recovery time varies for benign, cyst, and malignant. The recovery time for benign is  $0.48 \pm 0.24$  sec as the thermal conductivity of lipid goes from  $0.1 \text{ Wm}^{-1} \text{ K}^{-1}$  to  $0.3 \text{ Wm}^{-1} \text{ K}^{-1}$ . The recovery time for malignant is  $0.6 \pm 0.3$  sec shorter than

benign, and the thermal conductivity of the proteins present in the malignant varies from 0.2 W m<sup>-1</sup> K<sup>-1</sup>–0.3 W m<sup>-1</sup> K<sup>-1</sup>. However, it is necessary to collect many tissue samples to fully grasp the exact relationship between the thermal conductivity of proteins and lipids and cell density.

#### **IV. CONCLUSION**

We discovered some intriguing evidence from active pulsed thermography technique using formalin fixed oral samples. In all the samples, tumour tissue exhibits a high cellularity compared to benign and cyst tissue. The Thermal conductivity of the malignant, benign relies on the physiological element say proteins lipids. This suggests that APT can assist pathologists in making speedy and accurate cancer tissue diagnoses based on the clinical characteristics identified in the lesions under investigation. APT can be used as an experimental general approach for diagnosing oral cancer from excised tissues, and it is currently being investigated.

#### **ACKNOWLEDGMENTS**

The authors would like to thank the RAMS, IGCAR Department, Kalpakkam, for continuous support with equipment and encouragement.

#### **Authors Contribution:**

Conceptualization, S.S.J., K.A.S., M.M., Methodology, S.S.J., K.A.S., Writing—original draft preparation, S.S.J., Writing—review and editing, S.S.J., K.A.S., M.M., P.A.S., K.T.M., All authors have read and agreed to the published version of the manuscript.

**Data Availability Statement:** The data presented in this study are available on request from the corresponding author.

**Conflicts of Interest:** Authors declare no conflicts of interest.

**Funding:** Authors received no specific funding for this work.

**Ethical Approval:** The study was approved by institutional /regional/national ethics/committee/ethics board of SRMIST/1509/IEC/2018.

#### **REFERENCES**

1. C. Laprise, H. P. Shahul, S. A. Madathil et al., “Periodontal diseases and risk of oral cancer in Southern India: results from the HeNCe life study,” *International Journal of Cancer*, vol. 139, no.7, pp. 1512–1519, 2016. View at: [Publisher Site](#) | [Google Scholar](#)
2. A.C. Veluthattil, S. P. Sudha, S. Kandasamy, and S. V. Chakkalakkoombil, “Effect of hypofractionated, palliative radiotherapy on quality of life in late-stage oral cavity cancer: a

- prospective clinical trial,” *Indian Journal of Palliative Care*, vol. 25, pp. 383–390, 2019. View at: [Publisher Site](#) | [Google Scholar](#)
3. L. V. Galvão-Moreira and M. C. F. N. da Cruz, “Oral microbiome, periodontitis and risk of head and neck cancer,” *Oral Oncology*, vol. 53, pp. 17–19, 2016. View at: [Publisher Site](#) | [Google Scholar](#)
  4. K. R. Atanasova and Ö. Yilmaz, “Looking in the Porphyromonas gingivalis cabinet of curiosities: the microbium, the host and cancer association,” *Molecular Oral Microbiology*, vol. 29, no. 2, pp. 55–66, 2014. View at: [Publisher Site](#) | [Google Scholar](#)
  5. D. P. Almond and P. M. Patel, “Photothermal Science and Techniques”, Chapman and Hall, London, 1996.
  6. N. Tabatabaei, “Matched-filter thermography”, *Appl. Sci.*, vol. 8 no. 4, p. 581, 2018.
  7. D.C.G. De Veld, M.J.H. Witjes, H.J.C.M. Sterenborg, and J.L.N. Roodenburg, “The status of in vivo autofluorescence spectroscopy and imaging for oral oncology”, *Oral Oncol.*, vol. 41, pp. 117–132005, doi:10.1016/j.oraloncology.2004.07.007. [[PubMed](#)][[CrossRef](#)] [[Google Scholar](#)]
  8. M. Mascitti, G. Orsini, V. Tosco, R. Monterubbianesi, A. Balercia, A. Putignano, M. Procaccini, and A. Santarelli, “An overview on current non-invasive diagnostic devices in oral oncology”, *Front. Physiol.*, p. 9, 2018, doi: 10.3389/fphys.2018.01510. [[PMC free article](#)][[PubMed](#)] [[CrossRef](#)] [[Google Scholar](#)].
  9. I.T. Dascălu, “Histopathological aspects in oral squamous cell carcinoma”, *Open Access J. Dent. Sci.*, p. 3, 2018, doi: 10.23880/oajds-16000173. [[CrossRef](#)] [[Google Scholar](#)]
  10. N. A. Diakides, “Infrared Imaging: An Emerging Technology in Medicine,” *IEEE Eng. Med. Biol. Mag.*, vol. 17, no. 4, pp. 17–18, 1998, [[PubMed](#)] [[Google Scholar](#)]
  11. X. P. Maldague, *Nondestructive evaluation of materials by infrared thermography* (Springer Science & Business Media, 2012) [[Google Scholar](#)].
  12. C. Herman and M. P. Cetingul, “Quantitative visualization and detection of skin cancer using dynamic thermal imaging,” *J. Vis. Exp.* 51, e2679 (2011). [[PMC free article](#)] [[PubMed](#)] [[Google Scholar](#)]
  13. A. Renkielska, M. Kaczmarek, A. Nowakowski, J. Grudziński, P. Czapiewski, A. Krajewski and I. Grobelny, “Active dynamic infrared thermal imaging in burn depth evaluation,” *J. Burn Care Res.*, vol. 35, no. 5, pp. e294–e303, 2014,
  14. C. Stefanadis, C. Chrysohoou, D. B. Panagiotakos, E. Passalidou, V. Katsi, V. Polychronopoulos, P. K. Toutouzas, “Temperature differences are associated with malignancy on

lung lesions: a clinical study,” *BMC Cancer*, vol. 3, no. 1, p. 1, 2003,

15. J. Wang, K.-J. Chang, C.-Y. Chen, K.-L. Chien, Y.-S. Tsai, Y.-M. Wu, Y.-C. Teng, and T. T.-F. Shih, “Evaluation of the diagnostic performance of infrared imaging of the breast: a preliminary study,” *Biomed. Eng. Online*, vol. 9, no. 1, p. 3, 2010, [PMC free article] [PubMed] [Google Scholar].

16. J. F. Head, F. Wang, C. A. Lipari and R. L. Elliott, “The important role of infrared imaging in breast cancer,” *IEEE Eng. Med. Biol. Mag.*, vol. 19, no. 3, pp. 52–57, 2000. [PubMed] [Google Scholar].

17. A. I. Moropoulou and K. C. Labropoulos, *Non-destructive testing for accessing structural damage and interventions effectiveness for built culture heritage protection*, Human-Computer Interaction: Concepts, Methodologies, Tools, and Applications, Information resources management association USA, 2015.

18. S. T. Huth, et al., “Lock-in IR-thermography-A novel tool for material and device characterization”, *Indifusion and defect data part B solid state phenomena*, pp. 741-746, 2002.

19. D. Bates, G. Smith, D. Lu and J. Hewitt, “Rapid thermal non-destructive testing of aircraft components”, *Compos. B. Eng.*, vol. 31, pp. 175–85, 2000.

20. F. Ciampa, P. Mahmoodi, F. Pinto, and M. Meo, “Recent advances in active infrared thermography for non-destructive testing of aerospace components”, *Sensors*, vol. 18, p. 609, 2018.

21. H. N. Hutson, C. Kujawa, K. Eliceiri, P. Campagnola, and K. S. Masters, “Impact of tissue preservation on collagen fiber architecture”, *Biotech. Histochem.*, vol. 94, pp. 134–144, 2019.

22. H. Tran, et al. “Formalin fixation and cryosectioning cause only minimal changes in shape or size of ocular tissues”, *Sci. Rep.*, vol. 7, p. 12065, 2017.

23. Park, B. K. et al. “Thermal conductivity of biological cells at cellular level and correlation with disease state”, *J. Appl. Phys.*, vol. 119, p. 224701, 2016.

24. L. E. Bagge, H. N. Koopman, S. A. Rommel, W. A. McLellan, and D. A. McLellan, “Lipid class and depth-specific thermal properties in the blubber of the short-finned pilot whale and the pygmy sperm whale”, *J. Exp. Biol.*, vol. 215, pp. 4330–4339, 2012.

25. A. I. Baba, and C. Cătoi, *Comparative Oncology*, Publishing House of the Romanian Academy Bucharest, 2007.

26. S. Päufer, A. Zschunke, A. Khuen, and K. Keller, “Estimation of water content and water mobility in the nucleus and cytoplasm of *Xenopus laevis* oocytes by NMR microscopy”, *Magn. Reson. Imaging*, vol. 13, pp. 269–276, 1995.

27. Black, J., *Microbiology: Principles and Exploration*, John Wiley & Sons, New York, NY, USA, 8th edition, 2012.

28. S. Yamaguchi, Y. Fukushi, O. Kubota, T. Itsuji, T. Ouchi, and S. Yamamoto, "Origin and quantification of differences between normal and tumor tissues observed by terahertz spectroscopy," *Physics in Medicine and Biology*, vol. 61, no. 18, pp. 6808–6820, 2016. View at: [Publisher Site](#) | [Google Scholar](#)

29. F. Wahaia, I. Kasalynas, D. Seliuta et al., "Study of gastric cancer samples using terahertz techniques," *Proceedings of SPIE*, vol. 9286, Article ID 92864H, 2014. View at: [Publisher Site](#) | [Google Scholar](#)

30. C. A. Schneider, W. S. Rasband, and K. W. Eliceiri, "NIH Image to ImageJ: 25 years of image analysis," *Nature Methods*, vol. 9, no. 7, pp. 671–675, 2012. View at: [Publisher Site](#) | [Google Scholar](#)

31. S. Stella Jenifer Isabella, K. A. Sunitha, K. T. Magesh, Sridhar P. Arjunan, BalaPesala, "Investigation of Formalin-Fixed Tissue Optical Characteristics in the Range of 200–500 GHz Using Pulsed Terahertz Reflection Spectroscopy to Differentiate Oral Malignant, Benign, and Cyst", *Journal of Spectroscopy*, 2022, 10 pages. <https://doi.org/10.1155/2022/3627705> View at: [Publisher Site](#) | [Google Scholar](#)